THE PENNSYLVANIA STATE UNIVERSITY
SCHREYER HONORS COLLEGE

DEPARTMENT OF ELECTRICAL ENGINEERING

ELECTROSTATIC MODELING OF POWER TRANSMISSION LINES USING BOUNDARY ELEMENT METHODS

JIANG, YIFAN
SPRING 2014

A thesis
submitted in partial fulfillment
of the requirements
for baccalaureate degrees
in Electrical Engineering and Physics
with honors in Electrical Engineering

Reviewed and approved* by the following:

Jeffrey Mayer
Associate Professor of Electrical Engineering
Thesis Supervisor

John Mitchell
Professor of Electrical Engineering
Honors Adviser

* Signatures are on file in the Schreyer Honors College.

ABSTRACT

The electric field at the surface of a power transmission line is an important consideration in the design of the line, as it is related to the capacitance of the line and to the possible onset of corona. Historically, the electric field has been calculated using a model that is known to produce results with a small error but that is very simple to evaluate, even manually. With growing interest in compact high-power lines, for which even small errors are concern, and the availability of low-cost computing, it seems logical to develop more accurate models for the electric field surrounding overhead power transmission lines. Boundary element methods (BEMs) are well suited for this purpose, as the surrounding media is homogeneous and the length scale ratio between the separation and radius of the conductors is very large. Conventional BEMs that rely on a geometric discretization of boundaries into elements would be usable, but two alternatives are considered in this thesis. The first alternative is very simple to formulate but sacrifices accuracy (it is still more accurate than the standard model). It is based on approximating the affect of each element as if the element was reduced to a point source. The second alternative is more complicated to formulate but provides an excellent trade-off between accuracy and computational requirements. It is based on a Fourier series or modal discretization of the boundary instead of a geometric one. The accuracy of the two alternative methods is demonstrated using a two-conductor case for which an analytical solution is known. The Fourier series method is then applied to two practical problems: determining the capacitance of a cable and the electric field of a high-voltage power transmission line with bundled conductors.

TABLE OF CONTENTS

LIST OF FIGURES

LIST OF TABLES

Chapter 1

Introduction

Overhead power transmission lines remain critical components in today's electric power systems, as they are necessary to transport energy from large generating stations to consumers. In addition to their intended function, however, overhead transmission lines also influence their surroundings through electric and magnetic fields. For example, the magnitude of the electric field at the surface of the transmission line conductors can be high enough to ionize the neighboring air, as manifest by an observable corona. This has several undesirable results, including power dissipation (losses), audible noise, and an increased chance of flashover during lightning storms or switching operations.

To minimize these undesirable results, transmission line designers calculate the maximum magnitude of the electric field as they consider trade-offs among the size and arrangement of conductors. The mathematical models used for these calculations yield reasonably good estimates of the magnitude of the electric field but are not exact, because of two approximations made to simplify the models. First, the charge on each conductor is assumed to have a uniform distribution (tangentially). Second, the equipotential constraint at the boundary of a conductor is neglected when considering the potential due to any other conductor. For conventional transmission lines, the errors introduced by these approximations have been accepted, because the errors are typically small (a few percent or less) and the models can be evaluated readily, even manually. With increasing interest in compact high-power transmission lines and practically free computation, however, it is logical to examine more precise models.

In this thesis, various forms of the boundary element method (BEM) are derived to obtain electrostatic potential models for power transmission lines. The BEM is based on the notion that the solution to a boundary value problem for a Laplace equation can be expressed in terms of a boundary integral that can be evaluated for specified boundary conditions. In conventional BEM, the boundary is discretized or divided into elements. The entire boundary integral is then expressed as the sum of the integrals for these elements. In this way, evaluation of the boundary integral can be adapted to yield a good approximation for most boundary geometries and boundary conditions. In this work, an alternative discretization is explored. More specifically, since the boundary geometry is cylindrical, the boundary conditions are represented using Fourier series. This modal discretization is shown to yield better results with fewer "elements".

1.1 Physical and Mathematical Model

The typical power transmission line can be modeled as a set of long, cylindrical conductors that are arranged in parallel. Because the lines are very long, it is reasonable to consider two-dimensional models in a plane to which the line is normal. We choose a coordinate system in which the axes of the conductors are parallel to the *z*-axis, so the models are in the *x*-*y* plane.

To derive mathematical models of the power transmission lines, we start with Maxwell's equations in differential form:

$$\nabla \cdot \vec{E} = \frac{\rho}{\varepsilon_0} \tag{1.1}$$

$$\nabla \cdot \vec{B} = 0 \tag{1.2}$$

$$\nabla \times \vec{E} = -\frac{\partial}{\partial t}\vec{B} \tag{1.3}$$

$$\nabla \times \vec{B} = \mu_0 \vec{J} + \mu_0 \varepsilon_0 \frac{\partial}{\partial t} \vec{E} \tag{1.4}$$

This thesis focuses on the electrostatic case in free space. Consequently, Maxwell's equations can be simplified. Since the transmission line is comprised of conductors, and we are interested in an electrostatic field, all charge should be located on the surface of the conductors – there is no charge or field inside the conductors. Therefore, (1.1) can be simplified to

$$\nabla \cdot \vec{E} = 0 \tag{1.5}$$

If we define the electric potential (also known as voltage) applied on the power lines as *u*, then the relationship between the voltage and the electric field can be expressed as

$$\vec{E} = -\nabla u \tag{1.6}$$

Combining (1.5) and (1.6) yields

$$\nabla^2 u = 0 \tag{1.7}$$

If the voltage applied to the conductors is specified, (1.7) becomes a boundary value problem for a two-dimensional Laplace equation. The charge distribution can be analyzed from this boundary value problem.

1.2 Solution of boundary value problems for a Laplace equation

There are several methods to solve the boundary value problem of the Laplace equation derived in the previous section. In the special case of only two parallel, cylindrical conductors, there is an analytical solution. However, in the more common case where there are more than two conductors, no analytical solution is known, so numerical methods must be formulated. As a numerical method, boundary element method (BEM) is available for the boundary problem and is able to generate results with relatively high precision.

Two analytical methods are introduced in Chapter 2. Furthermore, different approaches of BEM are presented in Chapter 3 and Chapter 4.

Chapter 2

Two Conductor Case

In the special case where there are only two parallel cylindrical conductors, it is possible to express the surface charge distribution of the two conductors analytically. A popular and classical analytical method used in textbooks (for example, Hayt, *Engineering Electromagnetics* [1]) takes advantage of the equipotential circles on conductors to avoid dealing with differential equations. An alternative method is to place the two conductors in a bipolar coordinate system and solve the resulting model directly from the related differential equation.

2.1 Classical Derivation

Assume there are two infinitely long parallel cylindrical conductors in free space, the voltages on the conductors are specified and the surface charge distribution needs to be

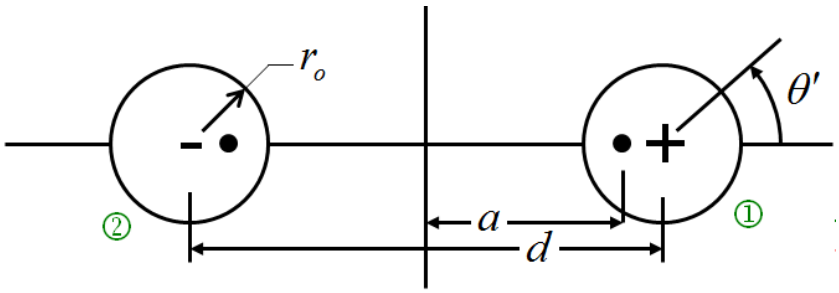

Figure 2-1. Two parallel conductors

calculated. The geometry of this problem is shown in Figure 2.1. The distance between the two conductors is d and the outer radius of each conductor is r_o. Now, imagine replacing the two parallel conductors with two parallel line charges each of which lies within the boundary of one of the original conductors. The line charges are parallel to the z axis and lie on the line connecting the centers of the original conductors at a distance a from the origin. Also, define the parallel axis and the vertical axis to be x-axis and y-axis respectively. For any point P with coordinate

(x, y), there is a potential, φ generated by the two line charges. If we denote the distance of point P to the two lines charges as r_1 and r_2, φ can be expressed by superposing the potential resulting from each line charge:

$$\varphi = -\frac{\lambda}{2\pi\varepsilon_0}\ln(r_1) + \frac{\lambda}{2\pi\varepsilon_0}\ln(r_2) \tag{2.1}$$

where λ is the linear charge density (i.e., charge per unit length along the line charge). Rearranging (2.1), yields the following relationship between r_1 and r_2 for an equipotential surface parameterized by a value for φ

$$\frac{r_2}{r_1} = \exp\left(\frac{2\pi\varepsilon_0}{\lambda}\varphi\right) \tag{2.2}$$

In Cartesian coordinate, (2.2) becomes

$$\frac{\sqrt{(x-a)^2 + y^2}}{\sqrt{(x+a)^2 + y^2}} = k \text{ , where } k = \exp\left(\frac{2\pi\varepsilon_0}{\lambda}\varphi\right) \tag{2.3}$$

Then, expand (2.3) to:

$$\left(x - \frac{k^2+1}{k^2-1}a\right)^2 + y^2 = \left(\frac{k^2+1}{k^2-1}\right)^2 a^2 - a^2 \tag{2.4}$$

Note that (2.4) corresponds to a function for a circle with the following center coordinates and radius

$$\left(\frac{k^2+1}{k^2-1}a,\ 0\right) \tag{2.5}$$

$$\sqrt{\left(\frac{k^2+1}{k^2-1}\right)a^2 - a^2} \tag{2.6}$$

Now, a and k can be expressed in terms of d and r_o, by enforcing the equipotential boundary condition for the original conductor. That is, the center coordinates and radius for the circular equipotential surface defined by (2.5) and (2.6) must coincide with the circular boundary of the

original conductor. Equating (2.5) to the center of the conductor $(\frac{1}{2}d, 0)$ and equating (2.6) to the radius of the conductor r_o, and then solving for a and k yields

$$a = \sqrt{(\tfrac{1}{2}d)^2 - r_o^{\,2}} \tag{2.7}$$

and

$$k = \frac{\frac{1}{2}d + a}{r_o}. \tag{2.8}$$

Combining the last two equations along the with the original expression for k given by (2.3), and then solving for φ yields

$$\varphi = \frac{\lambda}{2\pi\varepsilon}\cosh^{-1}\left(\frac{\frac{1}{2}d}{r_o}\right) \tag{2.9}$$

From (1.6), the electric field is just the negative gradient of the potential. Also, the surface charge density is equal to ε_0 times the magnitude of the electric field. Thus, expressing the magnitude of the gradient of equation (2.1) and substituting the expression for a in (2.9), the surface charge distribution of the left conductor, $\sigma(\theta')$ is:

$$\sigma(\theta') = \frac{\lambda}{2\pi}\frac{a}{r_o\left(\frac{1}{2}d - r_o\cos(\theta')\right)} \tag{2.10}$$

2.2 Bipolar Coordinate Derivation

As shown in the introduction section, the problem in Section 2.1 can be mathematically modeled as a boundary value problem for a Laplace equation:

$$\nabla^2\varphi = 0 \tag{2.11}$$

The boundary values of this problem are specified as the voltages applied on the conductors. The typical method to solve a boundary value problem can be applied if one uses bipolar coordinates, for which

$$x = \alpha \frac{\sinh \tau}{\cosh \tau - \cos \sigma} \tag{2.12}$$

$$y = \alpha \frac{\sin \sigma}{\cosh \tau - \cos \sigma} \tag{2.13}$$

where α is a constant and $\sigma \in [0, 2\pi]$, $\tau \in [-\infty, \infty]$ are the bipolar coordinates. In this coordinate system, the circular geometry of the two conductors can be represented as

$$x^2 + (y - \alpha \cot \sigma)^2 = \frac{\alpha^2}{\sin^2 \sigma} \tag{2.14}$$

$$(x - \alpha \coth \sigma)^2 + y^2 = \frac{\alpha^2}{\sinh^2 \tau} \tag{2.15}$$

where (2.14) and (2.15) correspond to the right conductor surface and the left conductor surface, respectively. Again, due to the symmetry, it is enough to consider only one conductor.

For further calculations, the value of α must be determined. The boundary conditions should be represented with respect to the bipolar coordinates as well. From (2.14), for the right conductor, it is a circle with origin at (αcothτ, 0) and radius r_o. Thus,

$$\tfrac{1}{2} d = \alpha \coth \tau \tag{2.16}$$

and

$$r_o = \frac{\alpha}{\sinh \tau} \tag{2.17}$$

Combining these two equations, α is determined as

$$\alpha = \sqrt{(\tfrac{1}{2} d)^2 - r_o^{\,2}} \tag{2.18}$$

and

$$\tau = \cosh^{-1} \frac{d}{a} \tag{2.19}$$

Since the surface of the right conductor is just the boundary with boundary value equal to the voltage applied on it,(2.19) defines the position of the boundary. Another important point is that

(τ, σ) corresponds to the *y*-axis if $\tau = 0$. Thus, there is another boundary condition: at $\tau = 0$, $\varphi = 0$ due to symmetry.

The preceding discussion recasts the boundary value problem in bipolar coordinates. Now, the Laplace equation in bipolar coordinates is:

$$\nabla^2 \varphi = \frac{1}{\alpha^2}(\cosh\tau - \cos\sigma)^2 \left(\frac{\partial^2 \varphi}{\partial \sigma^2} + \frac{\partial^2 \varphi}{\partial \tau^2} \right) = 0 \tag{2.20}$$

This boundary value problem can be solved by separation of variables. Details regarding the solution are given in [2]. The final expression for the charge density is

$$\sigma_R = \frac{\varepsilon_0 V_1 \sqrt{(\frac{1}{2}d)^2 - r_o^{\,2}}}{r_o(\frac{1}{2}d + r_o \cos\beta) \ln\left(\dfrac{\frac{1}{2}d}{r_o} + \sqrt{\dfrac{(\frac{1}{2}d)^2}{r_o^{\,2}} - 1} \right)} \tag{2.21}$$

where V_1 is the voltage applied on the right conductor and β is the angular position around the conductor.

The preceding derivation shows that the use of bipolar coordinates gives an alternative solution of the potential problem, but it requires considerable mathematical effort and is restricted to this special two-conductor case.

Chapter 3

Conventional Boundary Element Method

As mentioned in Chapter 1, the calculation of charge distributions on conductors is mathematically modeled as a two-dimensional Laplace equation. Here, we will consider N conductors. The potential applied to the n^{th} conductor is φ_n. On the boundary of the n^{th} conductor, the charge q_n corresponds to the negative normal derivative of the potential $-\partial\varphi_n / \partial n$. Thus, the Laplace equation corresponds to a boundary value problem with boundary conditions specified as φ_n and the value to be determine is q_n. The space inside the n^{th} conductor is the domain denoted as Ω_n, while the boundary of the n^{th} conductor is denoted as Γ_n.

For this type of potential problem, the Boundary Element Method can be applied to solve numerical results. The application of BEM is basically comprised of three parts: the fundamental solution of the Laplace equation, the boundary integration equation, and the discretization of boundaries.

3.1 Fundamental solution of the Laplace equation

The fundamental solution of a Laplace equation is defined as φ^* and satisfies (3.1), where P and Q are any points in the domain. Also, define P' and Q' such that they correspond to the points on the boundary.

$$\nabla^2\varphi^*(P,Q) + \delta(P-Q) = 0 \tag{3.1}$$

For a two-dimensional Laplace equation in free space, φ^* is given as

$$\varphi^* = \frac{1}{2\pi} In \frac{1}{r(P,Q)} \tag{3.2}$$

3.2 Boundary integral equation

From the boundary conditions, the value of φ is known. However, in the original form of the Laplace equation (1.7), q does not appear explicitly. Consequently, the Laplace equation must be transformed to relate φ and q. The transformation is analogous to the weak form of the Laplace equation, which is commonly used in the finite element method.

To transform the equation, we pre-multiply $\nabla^2\varphi$ by v and integrate. For convenience, we define the domain as $\Omega = \Omega_1 + \Omega_2 + ... + \Omega_N$ and the boundary as $\Gamma = \Gamma_1 + \Gamma_2 + ... + \Gamma_N$. Then, the integration can be expressed as

$$\int_{\Omega} v\nabla^2\varphi d\Omega = 0 \tag{3.3}$$

This equation can be rearranged to the following form

$$\int_{\Omega} v\nabla^2\varphi d\Omega = \int_{\Omega} \left[\frac{\partial}{\partial x}\left(v\frac{\partial\varphi}{\partial x}\right) - \frac{\partial v}{\partial x}\frac{\partial\varphi}{\partial x} + \frac{\partial}{\partial y}\left(v\frac{\partial\varphi}{\partial y}\right) - \frac{\partial v}{\partial y}\frac{\partial\varphi}{\partial y}\right] d\Omega \tag{3.4}$$

Based on divergence theorem, this equation can be arranged to

$$\int_{\Omega} v\nabla^2\varphi d\Omega = \int_{\Gamma} v\frac{\partial\varphi}{\partial n} d\Gamma - \int_{\Omega} \left(\frac{\partial v}{\partial x}\frac{\partial\varphi}{\partial x} + \frac{\partial v}{\partial y}\frac{\partial\varphi}{\partial y}\right) d\Omega \tag{3.5}$$

Similar,

$$\int_{\Omega} \varphi\nabla^2 v d\Omega = \int_{\Gamma} \varphi\frac{\partial v}{\partial n} d\Gamma - \int_{\Omega} \left(\frac{\partial\varphi}{\partial x}\frac{\partial v}{\partial x} + \frac{\partial\varphi}{\partial y}\frac{\partial v}{\partial y}\right) d\Omega \tag{3.6}$$

Combing (3.5) and (3.6) yields the equation commonly known as Green's function:

$$\int_{\Omega} (v\nabla^2\varphi - \varphi\nabla^2 v) d\Omega = \int_{\Gamma} \left(v\frac{\partial\varphi}{\partial n} - \varphi\frac{\partial v}{\partial n}\right) d\Gamma \tag{3.7}$$

It is important to realize that for the preceding derivation the functions v and φ must be differentiable in the domain and on the boundary. This requirement is naturally achieved for φ; however, to satisfy this requirement v cannot be arbitrary. Since the fundamental solution introduced in Section 3.1 is just an φ function, it is safe to use φ^* as the function v. Thus, substituting φ^* into (3.7) yields

$$\int_{\Omega} [\varphi^*(P,Q)\nabla^2\varphi(Q) - \varphi(Q)\nabla^2\varphi^*(P,Q)]\, d\Omega(Q) = \int_{\Gamma} [\varphi^*(P,Q')\nabla^2 q(Q') - \varphi(Q')\nabla^2 q^*(P,Q')]\, d\Gamma(Q') \tag{3.8}$$

In this equation, Q' means the point is on the boundary and q^* is the normal derivative of φ^*. Combining (3.1) and (3.8), an integral equation (3.9) is formulated to relate $\varphi(Q)$, $\varphi(Q')$ and $q(Q')$:

$$\varphi(P) = \int_{\Gamma} [\varphi^*(P,Q')q(Q') - \varphi(Q')q^*(P,Q')]\, d\Gamma(Q') \tag{3.9}$$

Since in the surface charge calculation problem, only the values on the boundaries are important, (3.9) must be adjusted so that all of the points are on the boundary. Substituting the fundamental solution into (3.9) and considering points on the boundary, the boundary integral is formulated as:

$$\frac{1}{2}\varphi(P') = \int_{\Gamma} [\varphi^*(P',Q')q(Q') - \varphi(Q')q^*(P',Q')]\, d\Gamma(Q') \tag{3.10}$$

The boundary integral equation gives a direct relationship between the specified potential (boundary condition) and the charge on the surface. The value of $q(Q')$ (the surface charge density) thus can be solved from the boundary integral equation.

3.3 Discretization of boundaries

There may be an analytical solution for (3.10) in some special cases, but in general, the equation must be evaluated numerically. In the surface charge calculation problem for multiple conductors, the equation can be solved by dividing the boundary into small elements and then approximating the integral on the entire boundary by the sum of the integrals on the small elements. This procedure is referred as boundary discretization. After the boundary discretization, it will be shown that the value of the surface charge density can be solved in a matrix form.

If the boundary geometry of the problem is arbitrary, there are several methods to approximate the boundary. Some examples are constant element and linear element. However, for the problem discussed in this thesis, the geometries of the boundaries are circles. Thus, the elements are arcs and it is possible to use theses arc elements in the integration.

Suppose the boundary is divided into *n* small elements, (3.10) can be discretized to

$$\frac{1}{2}\varphi(P_i') + \sum_{j=1}^{n} \varphi_j \int_{\Gamma_j} q^*(P_i', Q')\, d\Gamma(Q') = \sum_{j=1}^{n} q_j \int_{\Gamma_j} u^*(P_i', Q')\, d\Gamma(Q') \tag{3.11}$$

In equation (3.11), Γ_j is the j^{th} element and Q' is a point on the element. P'_i is called the node of the i^{th} element. Since on the conductors, the potentials are all the same on the boundary, it is relatively free to choose the node position. For implementation convenience, the node is chosen to be the mid-point on the i^{th} element.

Obviously, equation (3.11) result for a linear equation set combined with *n* linear equations. This point indicates that it is convenient to write equation (3.11) in matrix form. Define

$$\widehat{H_{ij}} = \int_{\Gamma_j} q^*(P_i', Q')\, d\Gamma(Q') \tag{3.12}$$

$$G_{ij} = \int_{\Gamma_j} \varphi^*(P_i', Q')\, d\Gamma(Q') \tag{3.13}$$

$$\delta_{ij} = \begin{cases} 0, & i \neq j \\ 1, & i = j \end{cases} \tag{3.14}$$

$$H_{ij} = \widehat{H_{ij}} + \frac{1}{2}\delta_{ij} \tag{3.15}$$

Then, equation (3.11) can be written as

$$\sum_{j=1}^{n} \varphi_j H_{ij} = \sum_{j=1}^{n} q_j G_{ij} \tag{3.16}$$

Or, in matrix form

$$\mathbf{HU = GQ} \tag{3.17}$$

where

$$U = \begin{pmatrix} \varphi_1 \\ \varphi_2 \\ \vdots \\ \varphi_n \end{pmatrix} \tag{3.18}$$

$$Q = \begin{pmatrix} q_1 \\ q_2 \\ \vdots \\ q_n \end{pmatrix} \tag{3.19}$$

The value of **U** is known from the specified boundary conditions and **Q** is the unknown surface charge distribution. To solve for **Q** from **HU** = **GQ**, it is only necessary to calculate the entries of the **H** and **Q** matrices.

3.4 Expressions for entries of H and G

The expressions for the entries of **H** and **G** depend on the discretization method. For discretization by small arcs, consider the circle in figure 3.1:

Figure 3-1. A small arc on the boundary

Suggest for the right circle with radius r_{oj}, the circle origin is denoted as (x_oj, y_{oj}). Qj is a point on an arc element which is the segment between point 1 and point 2. Moreover, define the central angle θ_j to be from the parallel position to the point Q_j. Thus, the position, (x,y) of Q_j can be represented as

$$x = x_{oj} + r_{oj}\cos(\theta_j) \tag{3.20}$$

$$y = y_{oj} + r_{oj}\sin(\theta_j) \tag{3.21}$$

Denote the position of P_i to be (x_i, y_i). The magnitude of the distance between P_i and Q_j is

$$|r| = \sqrt{(x - x_i)^2 + (y - y_i)^2} \tag{3.22}$$

Based on equation (3.12) and (3.13), H_{ij} and G_{ij} can be expressed as

$$H_{ij} = \int_{\theta_{j2}}^{\theta_{j1}} \frac{\partial \varphi}{\partial n} d\theta_j \tag{3.23}$$

$$G_{ij} = \int_{\theta_{j2}}^{\theta_{j1}} \varphi d\theta_j \tag{3.24}$$

To calculate the normal derivative of φ,

$$\frac{\partial \varphi}{\partial n} = \frac{\partial \varphi}{\partial r}\frac{\partial r}{\partial n} = \frac{1}{2\pi}\left(-\frac{1}{r}\right)\frac{\cos(\theta_j)(x - x_i) + \sin(\theta_j)(y - y_i)}{|r|} \tag{3.25}$$

Combine equation (3.14), (3.16) and (3.17), all of the entries in the **H** and **G** matrices can be calculated. Unfortunately, the integration in (3.24) cannot be simplified to be a concise formula. Therefore, the integral should be evaluated through numerical methods. As a numerical integration method, Gaussian quadrature should be an effective and simple way to solve the integrations.

Chapter 4

Alternative Boundary Element Methods

The method discussed in Chapter 3 provides a conventional numerical approach to calculate the surface charge distribution on power lines. However, the integrals in H_{ij} and G_{ij} entries must be solved numerically and therefore it decreases the effectiveness of calculation. Thus, to increase the calculation speed, it implies to avoid numerical integrations. In this chapter, two alternative boundary element methods are discussed to avoid numerical integrations.

To avoid numerical integration, there are basically two approaches. The first approach is to discretize the boundary as many points. A point can be considered as a "segment" with 0 length. When doing integrations along this "segment", the calculation becomes very simple. Another approach is to find a method to discretize the boundary such that the integrals can be solved analytically. As to be shown in this chapter, the boundary can be discretized as modes. After the modal discretization, a compact formulation of integrals obviates the need for numerical integration.

4.1 Point Method

Recall the problem shown in Section 2.1. Suggest the boundary is divided as N points. The potential at a position P due to any point on the boundary is

$$\varphi_k(x,y) \approx \frac{\lambda_k}{2\pi\varepsilon}\ln(r) \quad \text{where} \quad r = \sqrt{(x-x_k)^2 + (y-y_k)^2} \tag{4.1}$$

The position of the point on the boundary is denoted as (x_k, y_k) and the position of the field point is denoted as (x, y). λ_k is the charge density at point (x_k, y_k).

The potential at point *P* can be determined by superposition of potentials due to each element. If point *P* is at the boundary and denote the potential at this point as φ_i,

$$\varphi_i = \sum_{n=1}^{N} \varphi_n \tag{4.2}$$

Adjust equation (4.2) and write it in matrix form, where r_{1n} means the distance from point 1 to point n, r_{2n} means the distance from point 2 to point n and so forth.

$$\begin{bmatrix} \varphi_1 \\ \varphi_2 \\ \varphi_3 \\ \vdots \\ \varphi_N \end{bmatrix} = \frac{1}{2\pi\varepsilon} \begin{bmatrix} \ln(r_{11}) & \ln(r_{12}) & \cdots & \cdots & \ln(r_{1n}) \\ \ln(r_{21}) & \ln(r_{22}) & \cdots & \cdots & \ln(r_{2n}) \\ \vdots & \vdots & \vdots & \vdots & \vdots \\ \vdots & \vdots & \vdots & \vdots & \vdots \\ \ln(r_{N1}) & \ln(r_{N2}) & \cdots & \cdots & \ln(r_{NN}) \end{bmatrix} \begin{bmatrix} \lambda_1 \\ \lambda_2 \\ \lambda_3 \\ \vdots \\ \lambda_N \end{bmatrix} \tag{4.3}$$

Denote

$$\mathbf{\Phi} = \begin{bmatrix} \varphi_1 \\ \varphi_2 \\ \varphi_3 \\ \vdots \\ \varphi_N \end{bmatrix}, \ \mathbf{\Lambda} = \begin{bmatrix} \lambda_1 \\ \lambda_2 \\ \lambda_3 \\ \vdots \\ \lambda_N \end{bmatrix} \text{ and } K = \frac{1}{2\pi\varepsilon} \begin{bmatrix} \ln(r_{11}) & \ln(r_{12}) & \cdots & \cdots & \ln(r_{1n}) \\ \ln(r_{21}) & \ln(r_{22}) & \cdots & \cdots & \ln(r_{2n}) \\ \vdots & \vdots & \vdots & \vdots & \vdots \\ \vdots & \vdots & \vdots & \vdots & \vdots \\ \ln(r_{N1}) & \ln(r_{N2}) & \cdots & \cdots & \ln(r_{NN}) \end{bmatrix}$$

Then, equation (4.3) can be written as

$$\mathbf{\Phi} = \mathbf{K}\mathbf{\Lambda} \tag{4.4}$$

The values of all entries in $\mathbf{\Phi}$ are given as boundary conditions and the values of all entries in **K** can be calculated from the geometry of the conductors. The charge density at the *N* points can be calculated by solving for $\mathbf{\Lambda}$ in (4.4). As long as *N* is large enough, the charge density at the *N* points should represent a good approximation of the surface charge distribution.

However, notice that the diagonal entries of the matrix **K** correspond to the self-potential of a point. The value of the self-potential becomes infinity and therefore poses problems for calculation. Thus, it is necessary to determine an appropriate formulation for the self-potential.

To determine the self-potential at point k, first divide the boundary as *N* small arc elements such that the n points used above is the mid-point of each arcs. Consider the arc shown in Figure 4.1:

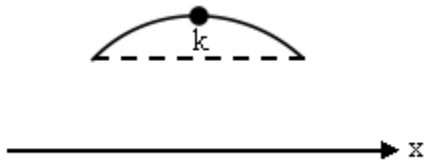

Figure 4-1. Self-potential on a small segment

Assume that this arc is very small and it can be approximated by a short straight line (the dashed line, and it is parallel to the x-axis in this case). Because the length of the line is also very small, the charge density can be considered as uniform. Thus, the charge distribution along the line is

$$\sigma_k = \frac{\lambda_k}{\Delta x} \tag{4.5}$$

Δx is the length of the line. The self-potential at the point k can be approximated by averaging the potential along the entire line. Combine equation (4.1) and (4.5) to calculate the potential at position x along the line:

$$
\begin{aligned}
\varphi_k(x) &= \int_{-\frac{1}{2}\Delta x}^{\frac{1}{2}\Delta x} \frac{1}{2\pi\varepsilon}\frac{\lambda_k}{\Delta x}\ln(|\xi - x|)d\xi \\
&= \frac{\lambda_k}{2\pi\varepsilon}\frac{1}{\Delta x}\left[\int_{-\frac{1}{2}\Delta x}^{x} \ln(x-\xi)d\xi + \int_{x}^{\frac{1}{2}\Delta x} \ln(\xi - x)d\xi\right] \\
&= \frac{\lambda_k}{2\pi\varepsilon}\frac{1}{\Delta x}\left[\left[-\left(\ln(x-\xi)-1\right)(x-\xi)\right]\Big|_{-\frac{1}{2}\Delta x}^{x} + \left[-\left(\ln(\xi - x)-1\right)(x-\xi)\right]_{x}^{\frac{1}{2}\Delta x}\right] \\
&= \frac{\lambda_k}{2\pi\varepsilon}\frac{1}{\Delta x}\left[\left(\ln\left(\tfrac{1}{2}\Delta x + x\right)-1\right)\left(\tfrac{1}{2}\Delta x + x\right) + \left(\ln\left(\tfrac{1}{2}\Delta x - x\right)-1\right)\left(\tfrac{1}{2}\Delta x - x\right)\right] \\
&= \frac{\lambda_k}{2\pi\varepsilon}\frac{1}{\Delta x}\left[\ln\left(\tfrac{1}{2}\Delta x + x\right)\left(\tfrac{1}{2}\Delta x + x\right) + \ln\left(\tfrac{1}{2}\Delta x - x\right)\left(\tfrac{1}{2}\Delta x - x\right) - \Delta x\right]
\end{aligned}
\tag{4.6}
$$

Then average the potential along the line to get the self-potential denoted as $\overline{\varphi}_k$:

$$
\begin{aligned}
\overline{\varphi}_k &= \frac{1}{\Delta x}\int_{-\frac{1}{2}\Delta x}^{\frac{1}{2}\Delta x} \varphi_k(x)dx \\
&= \frac{1}{\Delta x}\int_{-\frac{1}{2}\Delta x}^{\frac{1}{2}\Delta x} \frac{\lambda_k}{2\pi\varepsilon}\frac{1}{\Delta x}\left[\ln\left(\tfrac{1}{2}\Delta x + x\right)\left(\tfrac{1}{2}\Delta x + x\right) + \ln\left(\tfrac{1}{2}\Delta x - x\right)\left(\tfrac{1}{2}\Delta x - x\right) - \Delta x\right]dx \\
&= \frac{\lambda_k}{2\pi\varepsilon}\frac{1}{(\Delta x)^2}(\Delta x)^2\left(\ln(\Delta x) - \tfrac{3}{2}\right) \\
&= \frac{\lambda_k}{2\pi\varepsilon}\left(\ln(\Delta x) - \tfrac{3}{2}\right)
\end{aligned}
\tag{4.7}
$$

Fortunately, the formula of $\overline{\varphi}_k$ is very simple and only depends on the charge density and the length of the line. Thus, approximate the n^{th} arc element with a straight line and denote the length of the line as l_n. Therefore, the diagonal entries can be replaced from the self-potential and equation (4.3) is transformed to equation (4.8).

$$\begin{bmatrix} \varphi_1 \\ \varphi_2 \\ \varphi_3 \\ \vdots \\ \varphi_N \end{bmatrix} = \frac{1}{2\pi\varepsilon} \begin{bmatrix} \ln(l_1) - \frac{3}{2} & \ln(r_{12}) & \cdots & \cdots & \ln(r_{1n}) \\ \ln(r_{21}) & \ln(l_1) - \frac{3}{2} & \cdots & \cdots & \ln(r_{2n}) \\ \vdots & \vdots & \vdots & \vdots & \vdots \\ \vdots & \vdots & \vdots & \vdots & \vdots \\ \ln(r_{N1}) & \ln(r_{N2}) & \cdots & \cdots & \ln(l_1) - \frac{3}{2} \end{bmatrix} \begin{bmatrix} \lambda_1 \\ \lambda_2 \\ \lambda_3 \\ \vdots \\ \lambda_N \end{bmatrix} \tag{4.8}$$

4.2 Fourier Method

The point method discussed in section 4.1.1 can be easily implemented due to the entries in the **K** matrix has a very simple formulation. However, to increase the precision of the result, the number *N* needs to be large. To overcome this problem, a Fourier method is developed to discretize the boundary. In Fourier method, the boundary is not divided by small elements and therefore, it is not a real "discretization" of the boundary. Instead, the charge distribution is "discretized" by Fourier series.

Define he surface charge distribution of the nth conductor as σ_n, and define θ' as shown

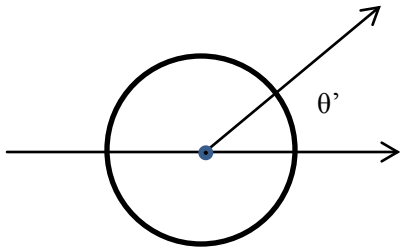

Figure 4-2. The definition of θ'

in figure 4.2. Let $\sigma_n = \sigma_n(\theta')$, an define the radius of the circle as r_{on}. Then from equation (4.1) and (4.2), the potential at (x,y) due to n conductors is therefore:

$$\varphi(x,y) = -\frac{1}{2\pi\varepsilon} \sum_{n=1}^{N} \int_{\theta'=0}^{2\pi} \sigma_n(\theta') \ln\left(\sqrt{[x-(x_n + r_{on}\cos(\theta'))]^2 + [y-(y_n + r_{on}\sin(\theta'))]^2} \right) r_{on}\, d\theta' \tag{4.9}$$

As a function of θ', σ_n can be written as a Fourier series:

$$\sigma_n(\theta') = \sum_{m=0}^{M} \left(\sigma_{nam}\cos(m\theta') + \sigma_{nbm}\sin(m\theta') \right) \tag{4.10}$$

If the value of *M* is infinity, equation (4.10) holds exactly. However, to implement the series, there is no way to use infinity for calculation. Nevertheless, it is still useful to assume that equation (4.10) is a modal form of the surface charge distribution function with some finite *M*. It is expected that for a larger *M*, the accuracy of the modal form is better.

Combine equation (4.9) and (4.10), the potential φ(x, y) can be represented as

$$\begin{aligned}\varphi(x,y) &= -\frac{1}{2\pi\varepsilon}\sum_{n=1}^{N}\int_{\theta'=0}^{2\pi}\sum_{m=0}^{M}\left(\sigma_{nam}\cos(m\theta')+\sigma_{nbm}\sin(m\theta')\right)\ln\left(\sqrt{[x-(x_n+r_{on}\cos(\theta'))]^2+[y-(y_n+r_{on}\sin(\theta'))]^2}\right)r_{on}d\theta' \\ &= -\frac{1}{2\pi\varepsilon}\sum_{n=1}^{N}\left[\int_{\theta'=0}^{2\pi}\sigma_{n0}\ln\left(\sqrt{[x-(x_n+r_{on}\cos(\theta'))]^2+[y-(y_n+r_{on}\sin(\theta'))]^2}\right)r_{on}d\theta'\right. \\ &\quad +\sum_{m=1}^{M}\int_{\theta'=0}^{2\pi}\sigma_{nam}\cos(m\theta')\ln\left(\sqrt{[x-(x_n+r_{on}\cos(\theta'))]^2+[y-(y_n+r_{on}\sin(\theta'))]^2}\right)r_{on}d\theta' \\ &\quad \left.+\sum_{m=1}^{M}\int_{\theta'=0}^{2\pi}\sigma_{nbm}\sin(m\theta')\ln\left(\sqrt{[x-(x_n+r_{on}\cos(\theta'))]^2+[y-(y_n+r_{on}\sin(\theta'))]^2}\right)r_{on}d\theta'\right]\end{aligned} \tag{4.11}$$

Notice that equation (4.11) is comprised of the sum of three integral equations. Fortunately, it turns out that the three integrations can be solved analytically and results in concise expressions. The calculation of the three integrals is shown in equation (4.12), (4.13) and (4.14) separately.

$$\int_{\theta'=0}^{2\pi}\ln\left(\sqrt{[x-(x_n+r_{on}\cos(\theta'))]^2+[y-(y_n+r_{on}\sin(\theta'))]^2}\right)d\theta' = \begin{cases} 0 & r_n \le r_{on} \\ 2\pi\ln\left(\dfrac{r_n}{r_{on}}\right) & r_n \ge r_{on} \end{cases} \quad \text{where} \quad r_n = \sqrt{(x-x_n)^2+(y-y_n)^2} \tag{4.12}$$

$$\int_{\theta'=0}^{2\pi} \cos(m\theta') \ln\left(\sqrt{[x-(x_n+r_{on}\cos(\theta'))]^2+[y-(y_n+r_{on}\sin(\theta'))]^2}\right) d\theta'$$

$$= \int_{\psi=\psi_a}^{\psi_a+2\pi} \ln\left(r_{on}\sqrt{1+\frac{r_n^2}{r_{on}^2}-2\frac{r_n}{r_{on}}\cos(\psi)}\right)\cos(m\psi-m\alpha_n)d\psi$$

$$= \int_{\psi=\psi_a}^{\psi_a+2\pi} \ln\left(r_{on}\right)\cos(m\psi-m\alpha_n)d\psi + r_o\int_{\psi=\psi_a}^{\psi_a+2\pi}\frac{1}{2}\ln\left(1+\frac{r_n^2}{r_{on}^2}-2\frac{r_n}{r_{on}}\cos(\psi)\right)\cos(m\psi-m\alpha_n)d\psi$$

$$= 0+\int_{\psi=\psi_a}^{\psi_a+2\pi}\frac{1}{2}\ln\left(1+\frac{r_n^2}{r_{on}^2}-2\frac{r_n}{r_{on}}\cos(\psi)\right)\left(\cos(m\psi)\cos(m\alpha_n)+\sin(m\psi)\sin(m\alpha_n)\right)d\psi$$

$$= \cos(m\alpha_n)\int_{\psi=\psi_a}^{\psi_a+2\pi}\frac{1}{2}\ln\left(1+\frac{r_n^2}{r_{on}^2}-2\frac{r_n}{r_{on}}\cos(\psi)\right)\cos(m\psi)d\psi + \sin(m\alpha_n)\int_{\psi=\psi_a}^{\psi_a+2\pi}\frac{1}{2}\ln\left(1+\frac{r_n^2}{r_{on}^2}-2\frac{r_n}{r_{on}}\cos(\psi)\right)\sin(m\psi)d\psi$$

$$= \cos(m\alpha_n)\left(-\frac{\pi}{m\left(\frac{r_n}{r_{on}}\right)^m}\right)+0$$

$$= -\pi\frac{\cos(m\alpha_n)}{m\left(\frac{r_n}{r_{on}}\right)^m} \qquad (4.13)$$

$$\int_{\theta'=0}^{2\pi} \sin(m\theta') \ln\left(\sqrt{[x-(x_n+r_{on}\cos(\theta'))]^2+[y-(y_n+r_{on}\sin(\theta'))]^2}\right) d\theta'$$

$$= \int_{\psi=\psi_a}^{\psi_a+2\pi} \ln\left(r_{on}\sqrt{1+\frac{r_n^2}{r_{on}^2}-2\frac{r_n}{r_{on}}\cos(\psi)}\right)\sin(m\psi-m\alpha_n)d\psi$$

$$= \int_{\psi=\psi_a}^{\psi_a+2\pi} \ln\left(r_{on}\right)\sin(m\psi-m\alpha_n)d\psi + r_o\int_{\psi=\psi_a}^{\psi_a+2\pi}\frac{1}{2}\ln\left(1+\frac{r_n^2}{r_{on}^2}-2\frac{r_n}{r_{on}}\cos(\psi)\right)\sin(m\psi-m\alpha_n)d\psi$$

$$= 0+\int_{\psi=\psi_a}^{\psi_a+2\pi}\frac{1}{2}\ln\left(1+\frac{r_n^2}{r_{on}^2}-2\frac{r_n}{r_{on}}\cos(\psi)\right)\left(\sin(m\psi)\cos(m\alpha_n)-\cos(m\psi)\sin(m\alpha_n)\right)d\psi$$

$$= \cos(m\alpha_n)\int_{\psi=\psi_a}^{\psi_a+2\pi}\frac{1}{2}\ln\left(1+\frac{r_n^2}{r_{on}^2}-2\frac{r_n}{r_{on}}\cos(\psi)\right)\sin(m\psi)d\psi - \sin(m\alpha_n)\int_{\psi=\psi_a}^{\psi_a+2\pi}\frac{1}{2}\ln\left(1+\frac{r_n^2}{r_{on}^2}-2\frac{r_n}{r_{on}}\cos(\psi)\right)\cos(m\psi)d\psi$$

$$= 0-\sin(m\alpha_n)\left(-\frac{\pi}{m\left(\frac{r_n}{r_{on}}\right)^m}\right)$$

$$= \pi\frac{\sin(m\alpha_n)}{m\left(\frac{r_n}{r_{on}}\right)^n} \qquad (4.14)$$

Use the results from equation (4.12), (4.13) and (4.14), equation (4.11) can be represented as

$$\varphi(x,y) = \frac{1}{2\pi}\sum_{n=1}^{N}\left[-\lambda_{n0}\delta_n(x,y)In(r_n) + \sum_{m=1}^{M}\left(\lambda_{nam}\frac{1}{2}\frac{\cos(m\alpha_n)}{m\left(\frac{r_n}{r_{on}}\right)^m}\right) + \sum_{m=1}^{M}\left(-\lambda_{nbm}\frac{1}{2}\frac{\sin(m\alpha_n)}{m\left(\frac{r_n}{r_{on}}\right)^m}\right)\right]$$

$$where\ \lambda_{n0} = \sigma_{n0}2\pi r_{on}$$

(4.15)

Similar to the point method, the Fourier method also formulates an equation that relates the potential and charge density at a point in the two-dimensional plane. Some sample points on the boundary can be chosen and written in a vector form:

$$\Phi = \begin{bmatrix}\varphi_1\\ \varphi_2\\ \varphi_3\\ \vdots\end{bmatrix}$$

Since for each φ in the vector, there is a corresponding equation that relates it to the charge density on that point as shown in equation (4.15), the charge distribution can be calculated by solving an equation similar to (4.4). If the **K** matrix is singular, least squares may be used to approximate the solution.

Chapter 5

Application of Methods to Transmission Problems

The discussion in Chapter 4 provides two boundary element methods that avoid the use of numerical integration for the problem of power transmission lines. It is important to check their accuracy though some simple application examples.

5.1 Two-Conductor Case

In the two conductor case, there are only two parallel transmission lines in free space, and as discussed in Chapter 2, there are analytical solutions. Therefore, the accuracy of the various BEMs can be checked by comparison to the analytical solutions.

The results of the charge density λ calculated by classical analytical method, point BEM and Fourier BEM are plotted in Figure 5.1. The number of elements is 1024 for the two numerical methods.

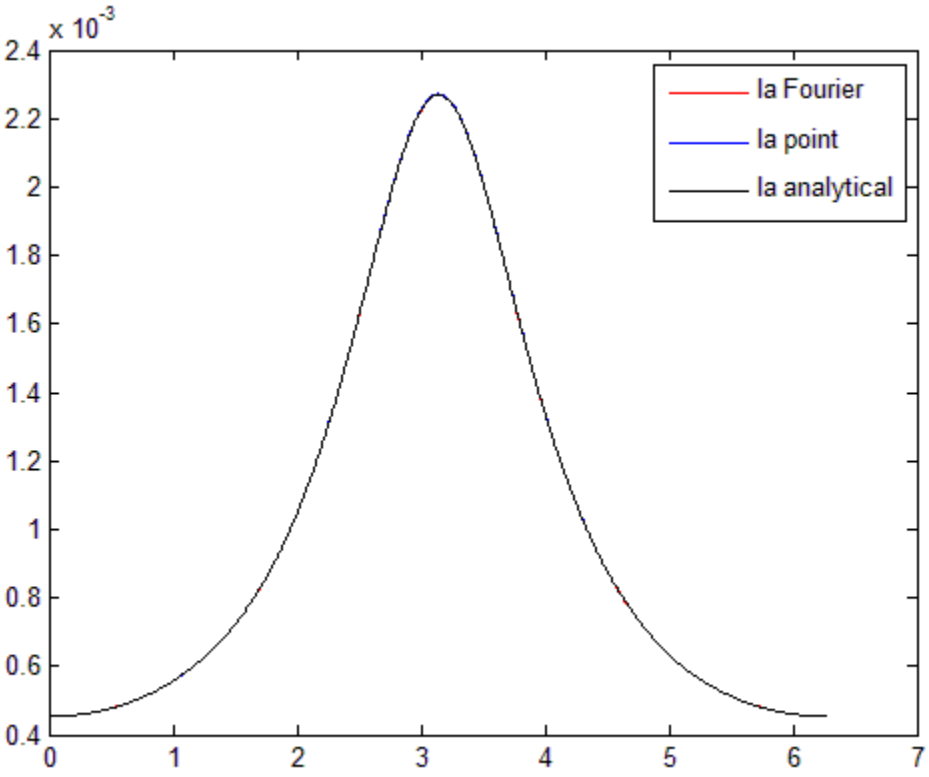

Figure 5-1. Charge density calculated by the three methods.

From figure 5-1, the plots of the three methods are nearly indistinguishable. It indicates that the error associated with the two BEMs is small. To get a more clear comparison, three-dimensional plots, Figure 5-2 and Figure 5-3, is generated for the error, the ratio of the distance and the conductors radius, as well as the number of elements.

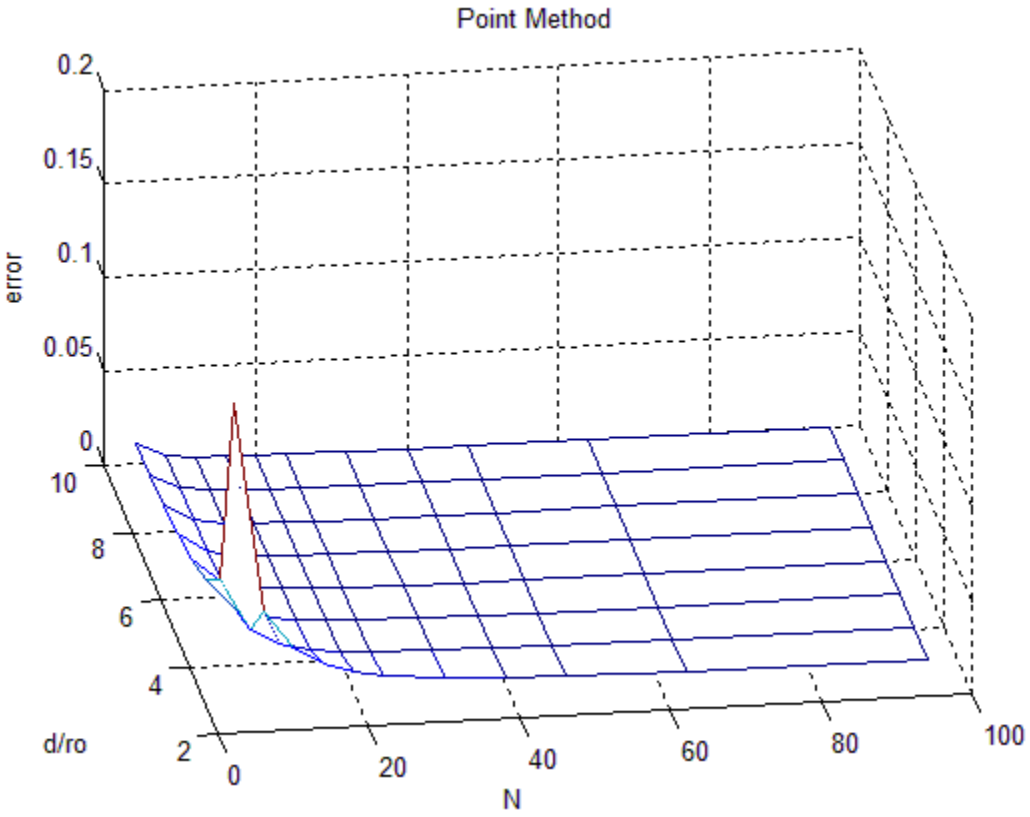

Figure 5-2. Three-dimensional plot of the point method

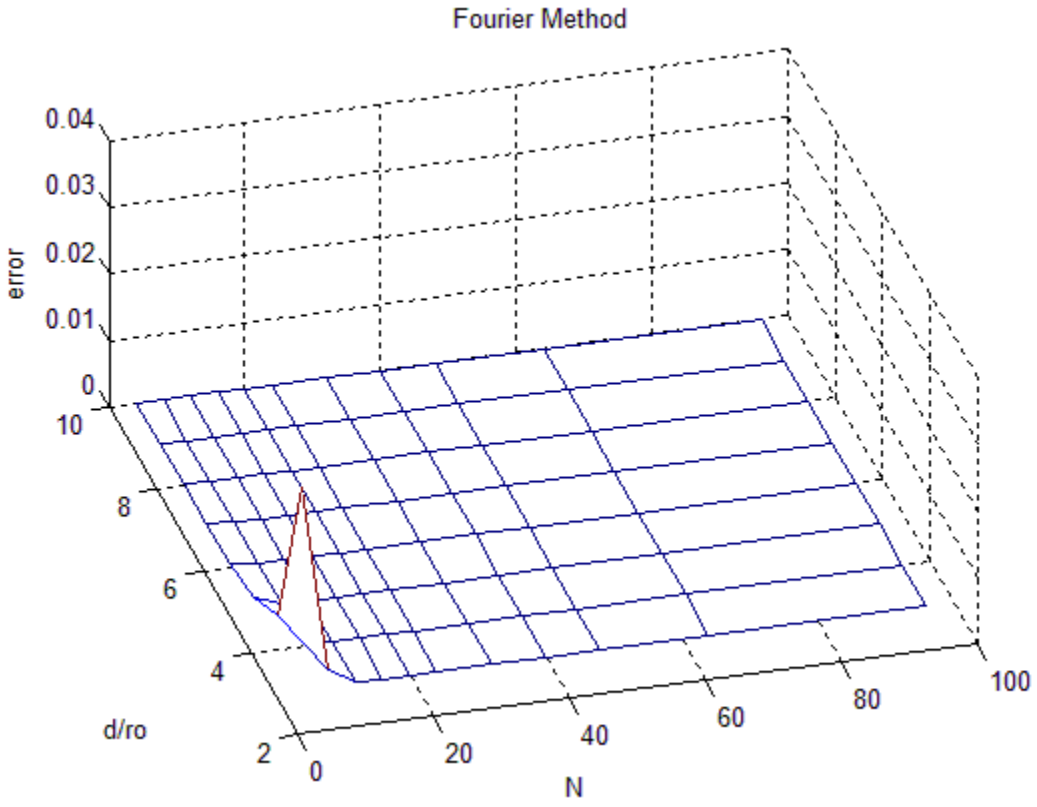

Figure 5-3. Three-dimensional plot of the Fourier method

From Figure 5-2 and Figure 5-3, it can be seen that the error converges to nearly zero when the number of elements or the d/r_o ratio is large. Moreover, for the Fourier method, the error is smaller than the error from the point method. The result from the Fourier method also converges faster than the result from point method. It is also valuable to notice that to get a good result, the number of element is not large for either of the two methods: 100 elements are enough to make the error be nearly zero. However, based the two figures, when the ratio of distance and radius is small, the error tends to be larger. Therefore, in real implementations, one should be more careful when setting the number of elements if the distance to conductor radius ratio is small. A large number of elements may be preferred.

5.2 Two-Cable Case

In real engineering applications, transmission lines are cables rather than cylindrical conductors. A cable is comprised of several cylindrical conductors or strands that are spiraled together. BEM can also be applied to analysis of such cables.

Figure 5-4 shows two cables in parallel. Each of the two cables is comprised of seven cylindrical conductors. For the right cable, 1 volt is to be applied, and for the left cable, -1 volt is to be applied.

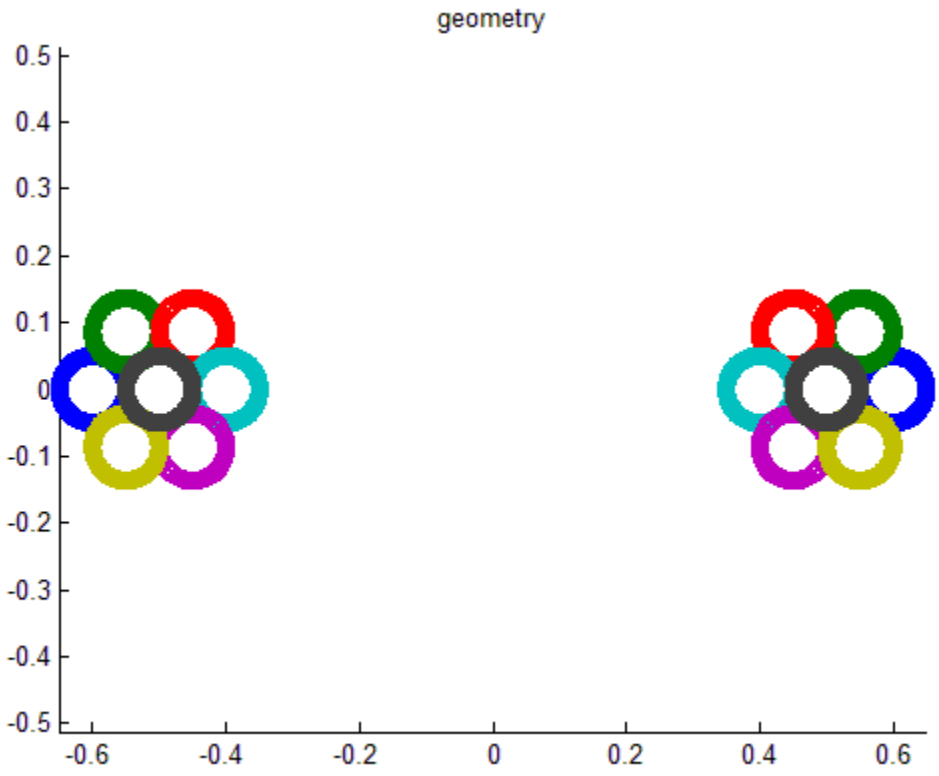

Figure 5-4. Two parallel cables.

The charge density of the bundled conductors for both of the two cables can be calculated by BEM. Figure 5-5 presents the result from Fourier method with 256 elements for each

conductor and 14 modes. Moreover, the three-dimensional plot of the potential is presented in Figure 5-6.

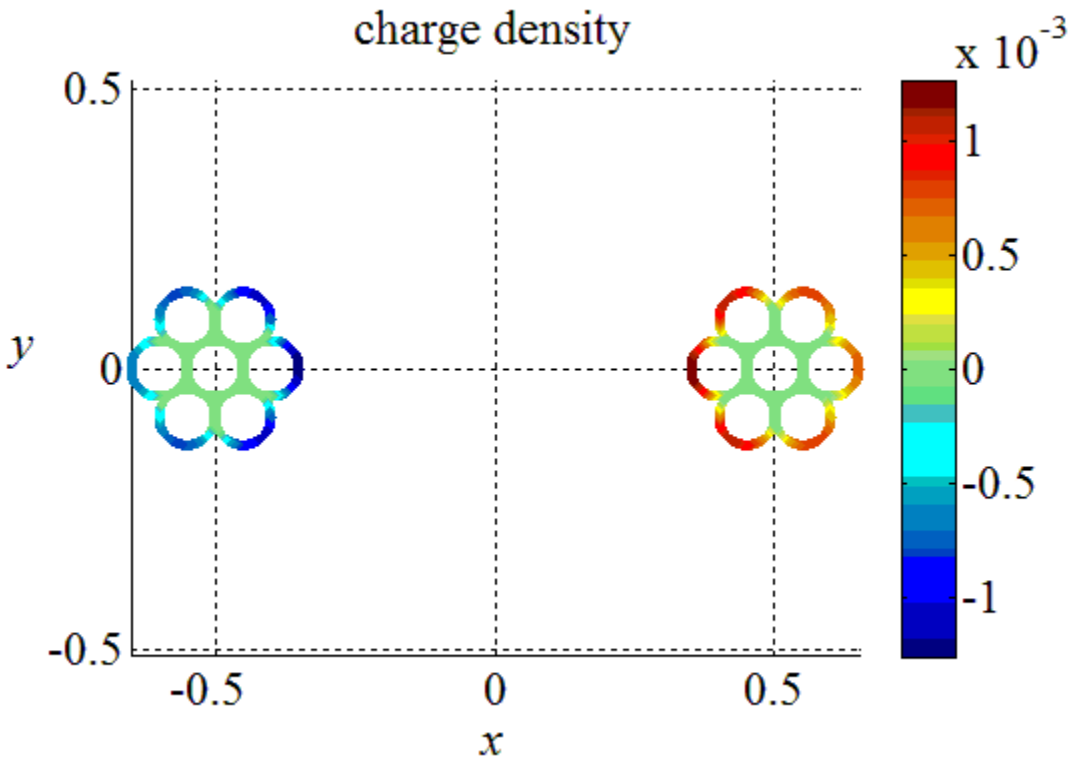

Figure 5-5. The charge density of two cables (without $\frac{1}{2\pi\epsilon_0}$.factor).

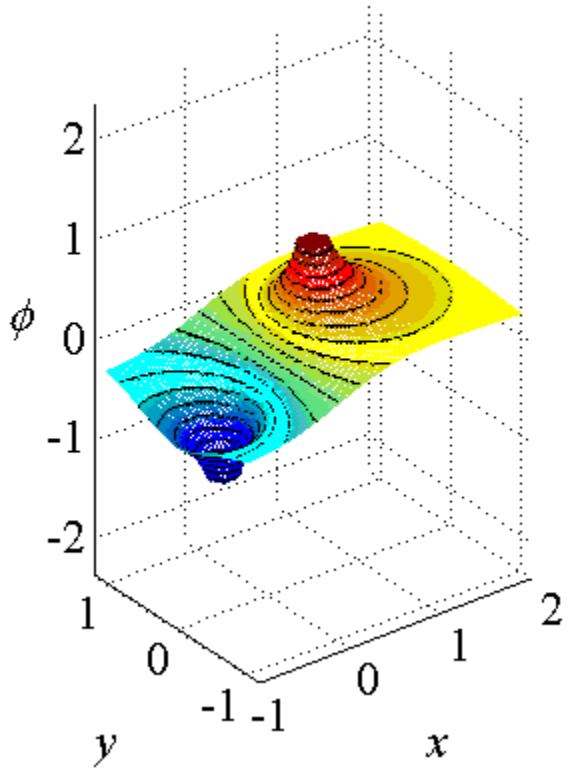

Figure 5-6. Three-dimensional plot of potential

It can be seen from Figure 5-5 and Figure 5-6 that if consider each of the two cables as one “big” conductor, the surface charge density is just similar for the case of only two parallel single conductors. Moreover, any boundaries corresponding to inner boundaries have a charge density of 0. That agrees with the discussion in the introduction chapter: for a perfect conductor, all of the charge should be placed on the out boundary.

For additional verification of the Fourier method, we apply it to a TransPowr® AAC Bare Overhead Conductor bundle to calculate the capacitance. The parameters of the conductor are shown in Table 5-1.

Table 5-1. Conductor Parameters [5]

CODE WORD	SIZE AWG OR kcmil	STRANDING NO. X DIA. INCHES	CLASS	CROSS SECTION SO. INCHES	GEOMETRIC MEAN RADIUS FT	CAPACITANCE MEGAOHM 100 FT (4)
Daisy	266.8	7x0.1953	AA	0.2095	0.0177	0.5815

The capacitance, C can be calculated from equation (5.1), where ω_e is the standard frequency used in U.S. and X'_a is the capacitive reactance for 1-foot spacing at 60 Hz in megaohm·1000 ft:

$$C = \frac{1}{\omega_e X a'} \tag{5.1}$$

Use BEM to calculate the charge distribution and the capacitance can be expressed as equation (5.2), where q is the amount of charge and V is the voltage applied on the conductor.

$$C = \frac{q}{V} \tag{5.2}$$

The charge distribution is in shown in Figure 5-7. The voltages applied on the cables are 1V and -1 V respectively. Fourier method is used with 256 elements and 14 modes. The distance and radius are not presented as the real implementation values but they are represented with the relative ratio.

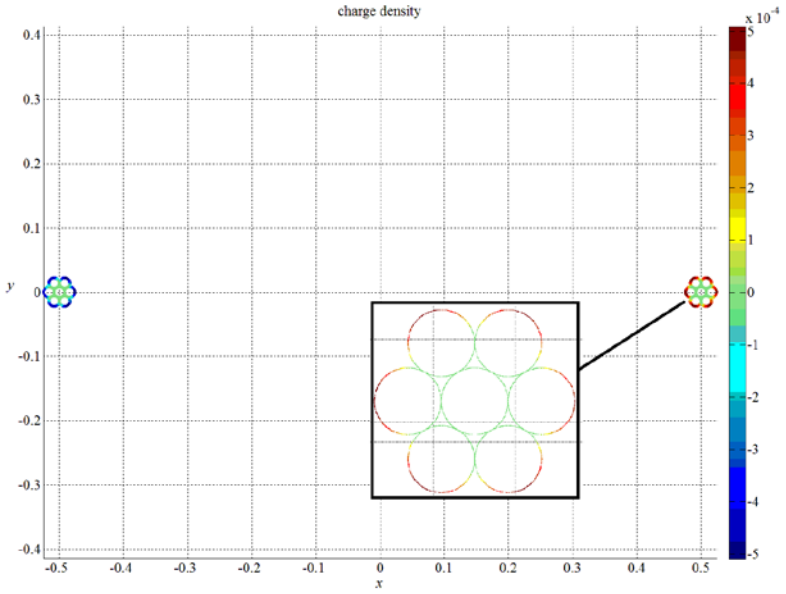

Figure 5-7. The charge density of two Daisy cables (without the $\frac{1}{2\pi\epsilon_0}$ $factor$)

The capacitance can also be estimated by using the geometry mean radius (GMR) of the cable:

$$V = \frac{1}{2\pi\varepsilon_0} In\left(\frac{1}{GMR}\right) q \tag{5.3}$$

The capacitance calculated from the specified conductor parameters, BEM and GMR are tabulated in Table 5-2. It can be seen that the capacitance calculated from the BEM is more close to the specified value than using GMR. The difference of the results between using BEM and specified values is within 10%.

Table 5-2. Capacitance

Method	Capacitance (pF)
Specified Parameters	14.966
BEM	13.706
GMR	16.805

5.3 Three-Phase Line with Bundled Conductors

The most commonly used transmission lines for power transmission have three phases. Figure 5-8 and 5-9 present two alternative designs for the 765-kV line recently constructed by AEP between Jackson Ferry, VA and Wyoming, WV. For this type of high-voltage power line, each phase is comprised of a bundle of cables. The Jackson Ferry-Wyoming line is the first in the United States to use a six-cable bundle; all previous transmission lines used four or fewer cables per bundle.

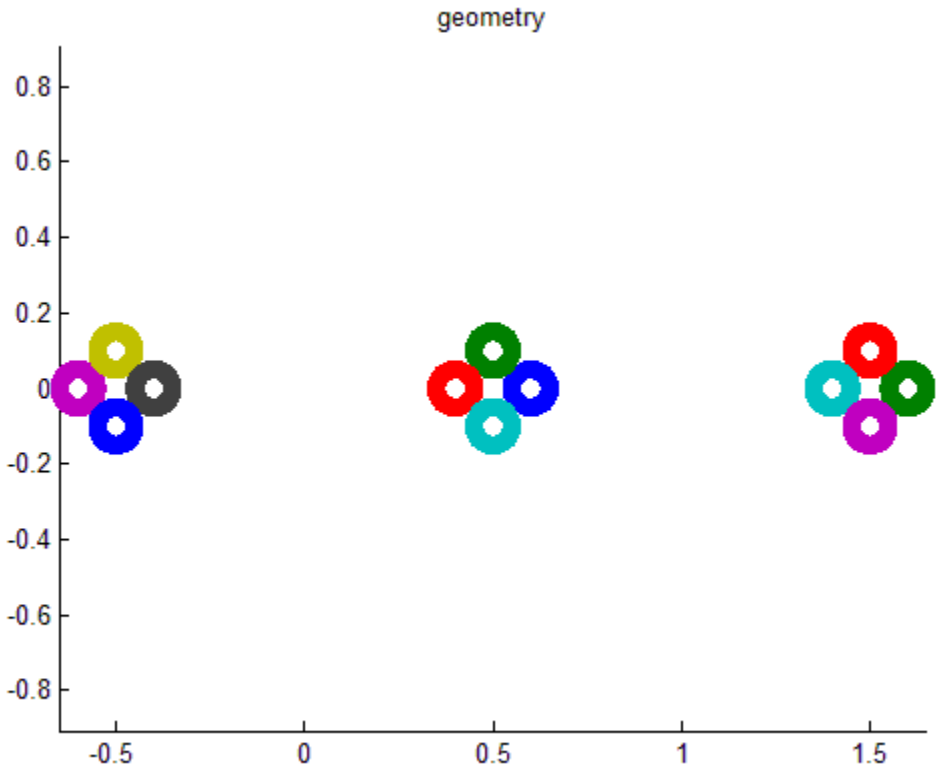

Figure 5-8. Three-phase transmission line with four-cable bundles.

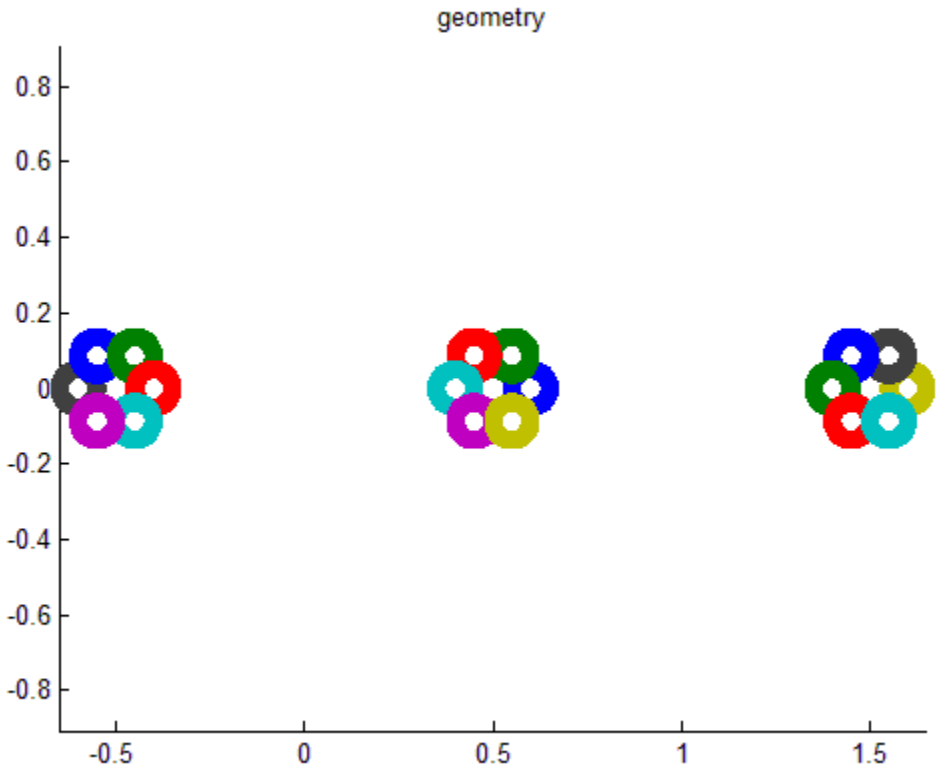

Figure 5-9. Three-phase transmission lines with six-cable bundles

As always, the charge density for each conductor can be solved by BEM. The Fourier method is used with 256 elements for each conductor and 14 modes. The results of the charge density and the three-dimensional plot are presented in Figure 5-10, 5-11, 5-12 and 5-13.

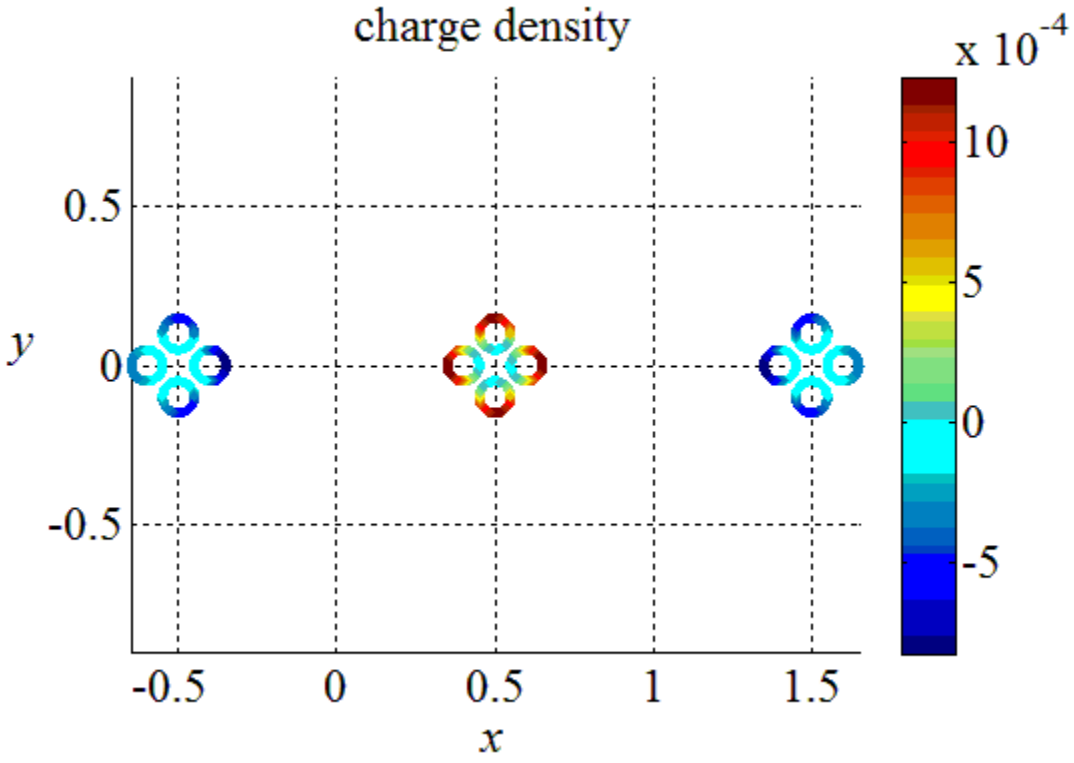

Figure 5-10. Charge density for four-cable bundle (without $\frac{1}{2\pi\epsilon_0}$ factor).

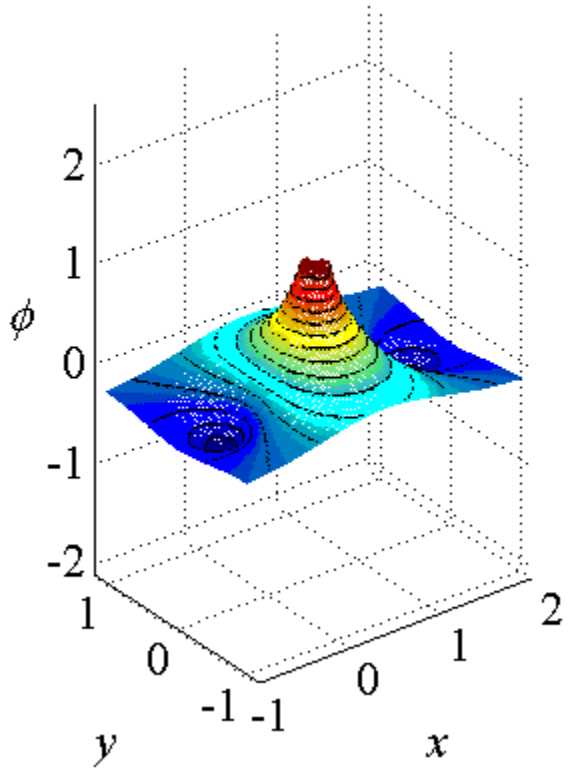

Figure 5-11. Three-dimensional plot of potential for four-cable bundle.

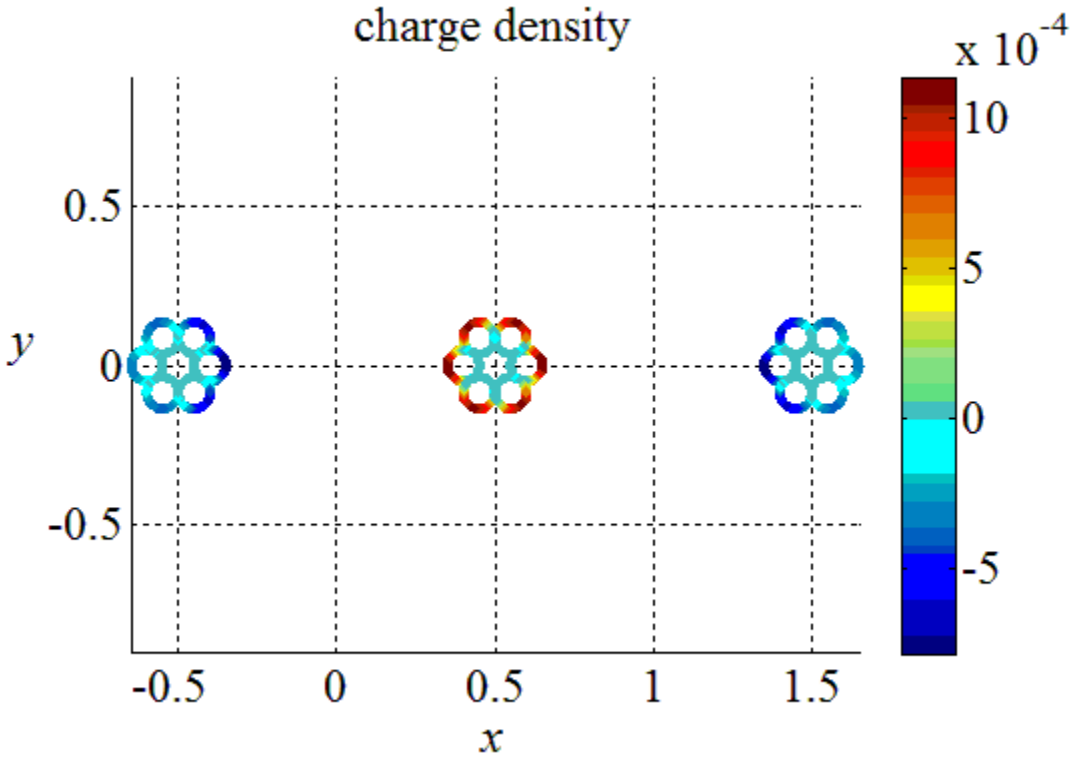

Figure 5-12. Charge density for six-cable bundles (without $\frac{1}{2\pi\epsilon_0}$ factor).

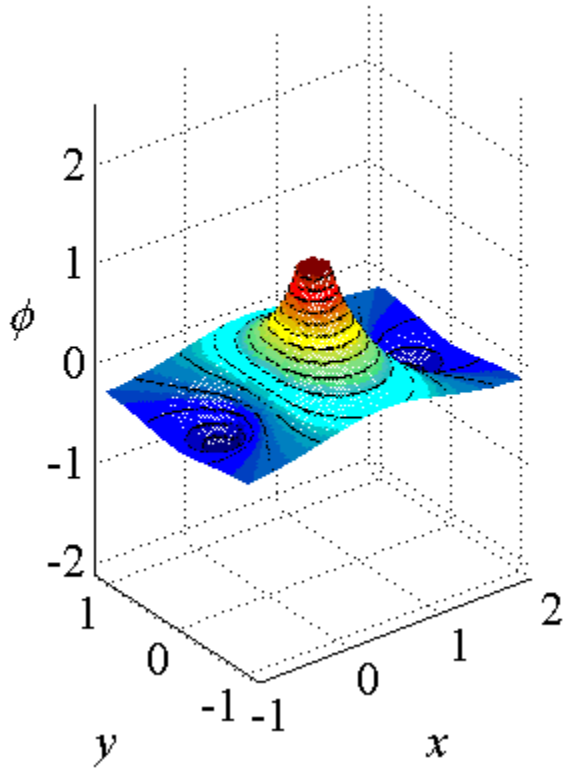

Figure 5-13. Three dimensional plot of potential for six-cable bundle.

The actual potential applied on the Jackson Ferry-Wyoming lines is 765 kV and the distance between neighboring phases is larger than shown in Figures 5-8 through 5-13t. After adjusting the applied potential and distance, the results are shown in Figure 5-14.

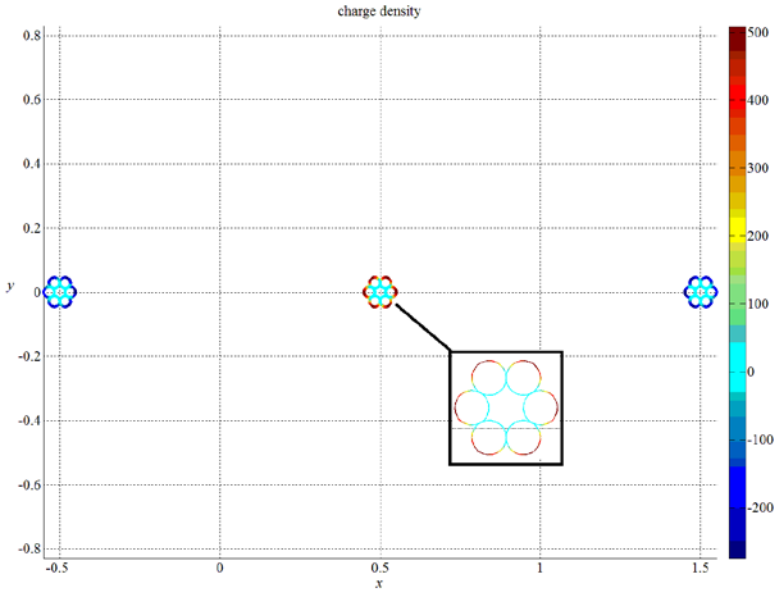

Figure 5-14. . Charge density six-cable bundle at 765 kV (without $\frac{1}{2\pi\epsilon_0}$ factor)

Based on the charge distribution, the electric field around the transmission lines can be calculated. The evaluation of electric field is useful for some safety issues, for example, corona discharge.

Chapter 6

Conclusions and Future Work

The boundary element method provides a useful approach to solve for charge distribution on power transmission lines. The Fourier series or modal discretization is especially attractive as it provides very good to excellent accuracy with a relatively small number of “elements”.

In this thesis, only the case in free space is discussed. Extending the results to include ground would be desirable. This needs to find the corresponding fundamental solution of the Laplace equation and the corresponding equation for the potential at a point on the plane.

BIBLIOGRAPHY

[1] Hayt, William Hart, Buck,John A. 2012. *Engineering electromagnetics*. New York, NY: McGraw-Hill

[2] Kristof Engelen, Pieter Jacqmaer and Johan Driesen (2013). Electric and magnetic fields of two infinitely long parallel cylindrical conductors carrying a DC current. *The European Physical Journal Applied Physics*, 64, 24515 doi:10.1051/epjap/2013120441.

[3] Wang, Yuanchun. 1988. *BianJie YuanFa JiChu*. Shang Hai, China: The publisher of Shanghai Jiao Tong University

[4] C.A. Brebbia, J. Dominguez, Boundary element methods for potential problems, *Applied Mathematical Modelling*, Volume 1, Issue 7, December 1977, Pages 372-378, ISSN 0307-904X, http://dx.doi.org/10.1016/0307-904X(77)90046-4. (http://www.sciencedirect.com/science/article/pii/0307904X77900464)

[5] General Cable. (2003). *TransPowr® Bare Overhead Conductors for Transmission and Distribution* [Online]. Available: http://www.stabiloy.com/NR/rdonlyres/5FFCCF8A-8706-4FE5-9C9D-CFD2DEEAEDB2/0/SEC4_Overhead_Conductors.pdf

[6] J. Mayer. Private calculation

ACADEMIC VITA

Yifan Jiang
637B WAUPELANI DRIVE, STATE COLLEGE, PA 16801 / yvj5043@psu.edu

EDUCATION

Pennsylvania State University, University Park (PSU) 2010 - Present
- Bachelor of Science in Electrical Engineering
- Bachelor of Science in Physics

ACADEMIC HONORS & AWARDS

Schreyer Honors College, PSU 2012 - Present
Bert Elsbach Honors Scholarship in Physics, PSU Fall 2012 - Spring 2013
Donald & Barbara Weyenberg Graduate Fellowship, PSU Fall 2012 - Spring 2013
The President's Freshman Award,PSU 2010

RESEARCH EXPERIENCE

Boundary Element Analysis of Power Lines PSU
Supervisor: Jeffrey Mayer, Thesis adviser: John Mitchell Sep.2013 – Present
- Model the power lines as two cylindrical conductors with dc currents. Write a MATLAB code that calculates the surface charge distribution of the power lines using boundary element analysis.
- Compare the results of numerical analysis with the analytical solution.
- Expand the method to more than two conductors; build a more general boundary element analysis model to calculate the surface charge distribution of n power lines in vacuum.

Finite Element Analysis of 1-D Nonhomogeneous Helmholtz Equation PSU
Supervisor: Anna Mazzucato Sep.2013 - Present
- Build the weak form of a 1-D Helmholtz equation.
- Choose available test functions. Solve the Helmholtz equation by finite element analysis using MATLAB.
- The nonhomogeneous term is approached by Fourier transformation.
- Analyze the wave equation through the Helmholtz equation.

ADDITIONAL INFORMATION

Computer Skills: MATLAB, Labview, SolidWorks and Comsol for modeling and simulation; programming with C++ and other languages
Language: Chinese (Native Speaker); English (Good);